C. R. Mecanique 343 (2015) 77–94

Contents lists available at ScienceDirect

Comptes Rendus Mecanique

www.sciencedirect.com

Mechanics of granular and polycrystalline solids

New three-dimensional plastic potentials for porous solids with a von Mises matrix

Oana Cazacu *, Benoit Revil-Baudard

Department of Mechanical and Aerospace Engineering, University of Florida, REEF, 1350 N. Poquito Rd., Shalimar, FL 32579, USA

ARTICLE INFO

Article history:
Received 14 January 2014
Accepted 26 April 2014
Available online 8 January 2015

Keywords:
Three-dimensional strain rate potentials
Three-dimensional stress-based potentials
Porous Mises solid
Coupled effects of stress invariants

ABSTRACT

In this paper, new 3-D plastic potentials for a porous solid with a von Mises matrix are obtained. First, a strain rate based potential is derived, the noteworthy result being its centro-symmetry. Moreover, it is revealed that the couplings between invariants are very specific, the most important influence of the third invariant being for axisymmetric states. It is demonstrated that the exact stress-based potential of the porous material should have the same key properties. Furthermore, it is deduced a new analytic 3-D stress-based potential that satisfies these properties. Compared to the existing criteria for porous solids with a von Mises matrix, this model is the only one that captures the specific couplings between all stress invariants and is exact for axisymmetric states.

1. Introduction

The most widely used criterion for porous solids containing randomly distributed spherical voids was developed by Gurson [1]. It is expressed as:

$$\Phi = \left(\frac{\Sigma_e}{\sigma_T}\right)^2 + 2f\cosh\left(\frac{3\Sigma_m}{2\sigma_T}\right) - 1 - f^2 = 0 \tag{1}$$

where f is the porosity, Σ_e is the von Mises effective stress, Σ_m is the mean stress, and σ_T is the tensile yield stress of the matrix. This model was deduced by performing limit-analysis of a hollow sphere made of a rigid-plastic material obeying von Mises criterion.

Modifications of criterion (1) were proposed based on finite-element (FE) studies (e.g., [2]) or using more complex trial velocity fields (e.g., [3]).

It is worth pointing out that Gurson's criterion (Eq. (1)) and all its modifications are expressed by functions that are invariant with respect to both transformations $(\Sigma_m, \boldsymbol{\Sigma}') \to (\Sigma_m, -\boldsymbol{\Sigma}')$ and $(\Sigma_m, \boldsymbol{\Sigma}') \to (-\Sigma_m, \boldsymbol{\Sigma}')$, where $\boldsymbol{\Sigma}'$ denotes the stress deviator. Furthermore, the effects of the mean stress and that of the stress deviator are decoupled. However, FE cell calculations (e.g., [4,5]) have shown that the stress triaxiality, $T = \Sigma_m/\Sigma_e$, by itself is insufficient to characterize yielding of a porous von Mises material. Moreover, the numerical results showed that the dilatational response displays a slight dependence on the third invariant of the stress deviator $J_3^{\Sigma} = \mathrm{tr}(\boldsymbol{\Sigma}'^3)/3$.

Recently, results of axisymmetric FE cell calculations [6] as well as full-field calculations of the yield surface of voided polycrystals deforming by slip at single crystal level [7] have revealed a very specific dependence of yielding with the signs

* Corresponding author: Tel.: +1 850 833 9350; fax: +1 850 833 9366.
E-mail address: cazacu@reef.ufl.edu (O. Cazacu).

http://dx.doi.org/10.1016/j.crme.2014.12.001
1631-0721/

of the mean stress and that of J_3^{Σ}. Specifically, for axisymmetric tensile loadings, the response corresponding to $J_3^{\Sigma} \geq 0$ is softer than that corresponding to $J_3^{\Sigma} \leq 0$, while for axisymmetric compressive loadings, the reverse occurs. Very recently, Cazacu et al. [8] explained these unusual features of the dilatational response under axisymmetric loadings and furthermore developed an analytical stress-based criterion that accounts for the coupled effects of the mean stress and third invariant of the stress deviator. Comparison between the predictions of this criterion and FE cell calculations also demonstrated that the model accounts for the role of the sign of the third invariant on void growth and collapse (see [5]). Another important outcome of the study of Cazacu et al. [8] was to show that the insensitivity of Gurson's [1] criterion to J_3^{Σ} is due to an approximation that Gurson made when calculating the overall plastic dissipation.

In this paper, new three-dimensional (3-D) potentials for a porous solid with a von Mises matrix are derived. The structure of the paper is as follows. We begin with a brief presentation of the kinematic homogenization approach of Hill–Mandel [9,10] that will be used for the derivation of the respective plastic potentials. An estimate of the strain rate based plastic potential of the porous material is provided. The limit-analysis is conducted for general 3-D conditions for both tensile and compressive states. To fully assess the couplings between all invariants, the shapes of its cross-sections with the octahedral plane are analyzed. Very specific couplings between all invariants are revealed. The noteworthy result obtained is that the shape of the cross-section of this potential with deviatoric planes (i.e. planes having the normal along the hydrostatic axis) changes little with the mean strain rate. Furthermore, the most pronounced influence of the third invariant occurs for axisymmetric states. An analytic strain rate based potential that satisfies all these key properties is proposed (Section 2). Furthermore, it is established that the stress-based potential of the porous material ought to satisfy the same properties of centro-symmetry with respect to the origin (Section 3). On this basis, we propose a new 3-D yield criterion for a porous Mises material. We also examine the corrections brought by this new yield criterion with respect to Gurson's (Eq. (1)). Further discussion and a summary of the main findings of this study are given in Section 4.

Regarding notations, vector and tensors are denoted by boldface characters. If $\mathbf{A}$ and $\mathbf{B}$ are second-order tensors, the contracted tensor product between such tensors are defined as: $\mathbf{A} : \mathbf{B} = A_{ij}B_{ij}i,\ j = 1 \ldots 3$; "tr" denotes the trace of the tensor.

2. Statement of the problem

Consider a representative volume element Ω, composed of a homogeneous rigid-plastic matrix and a traction-free void. For spherical void geometry an appropriate representative volume element (RVE) is a hollow sphere. Let a denote its inner radius and b its outer radius. The void volume fraction f is defined as $f = a^3/b^3$. The matrix material is described by a convex yield function $\varphi(\boldsymbol{\sigma})$ in the stress space and an associated flow rule:

$$\mathbf{d} = \dot{\lambda}\frac{\partial \varphi}{\partial \boldsymbol{\sigma}} \tag{2}$$

where $\boldsymbol{\sigma}$ is the Cauchy stress tensor, $\mathbf{d} = \frac{1}{2}(\nabla \mathbf{v} + \nabla \mathbf{v}^{\mathrm{T}})$ denotes the strain rate tensor with $\mathbf{v}$ being the velocity field, and $\dot{\lambda} \geq 0$ stands for the plastic multiplier rate. The yield surface is defined as $\varphi(\boldsymbol{\sigma}) = \sigma_{\mathrm{T}}$, where σ_{T} is the uniaxial yield in tension. Let's denote by C the convex domain delimited by the yield surface such that

$$C = \left\{\boldsymbol{\sigma} \;\middle|\; \varphi(\boldsymbol{\sigma}) \leq 0\right\}$$

The plastic dissipation potential of the matrix is defined as

$$\pi(\mathbf{d}) = \sup_{\boldsymbol{\sigma} \in C}(\boldsymbol{\sigma} : \mathbf{d}) \tag{3}$$

For uniform strain rate boundary conditions on $\partial\Omega$ i.e.

$$\mathbf{v} = \mathbf{D}\mathbf{x}, \quad \text{for any } \mathbf{x} \in \partial\Omega \tag{4}$$

with $\mathbf{D}$, the macroscopic strain rate tensor, being constant, Hill–Mandel [9,10] lemma applies; hence,

$$\langle \boldsymbol{\sigma} : \mathbf{d} \rangle_{\Omega} = \boldsymbol{\Sigma} : \mathbf{D} \tag{5}$$

where $\langle\rangle$ denotes the average value over the representative volume Ω, and $\boldsymbol{\Sigma} = \langle \boldsymbol{\sigma} \rangle_{\Omega}$. Furthermore, there exists a strain rate potential (SRP) for the porous material,

$$\Pi(\mathbf{D}) = \inf_{\mathbf{d} \in K(\mathbf{D})} \left\langle \pi(\mathbf{d}) \right\rangle_{\Omega} \tag{6a}$$

So using Eq. (5), the macroscopic stress tensor is expressed as:

$$\boldsymbol{\Sigma} = \frac{\partial \Pi(\mathbf{D}, \mathrm{f})}{\partial \mathbf{D}} \tag{6b}$$

In Eq. (5), $K(\mathbf{D})$ is the set of incompressible velocity fields satisfying condition (3) (for more details, see [11]).

This result will be further used for the derivation of the strain rate potential for a porous Mises material containing randomly distributed spherical voids.

2.1. New analytic strain rate potential for a porous solid with a von Mises matrix

If the matrix of the porous material is governed by the von Mises criterion, i.e. in Eq. (2) $\varphi(\boldsymbol{\sigma}) = \sqrt{(3/2)\boldsymbol{\sigma}' : \boldsymbol{\sigma}'}$, $\boldsymbol{\sigma}'$ being the stress deviator, then the local plastic dissipation is:

$$\pi(\mathbf{d}) = \sigma_T \sqrt{(2/3)\mathbf{d} : \mathbf{d}} \tag{7}$$

The analysis will be conducted for general 3-D loadings for both tensile and compressive states, i.e.

$$D = D_1 \mathbf{e}_1 \otimes \mathbf{e}_1 + D_2 \mathbf{e}_2 \otimes \mathbf{e}_2 + D_3 \mathbf{e}_3 \otimes \mathbf{e}_3 \tag{8}$$

with D_1, D_2, D_3 being the eigenvalues (unordered) of $\mathbf{D}$ and ($\mathbf{e}_1$, $\mathbf{e}_2$, $\mathbf{e}_3$) its eigenvectors.

As in Gurson [12,1], we use the trial velocity field $\mathbf{v}$, deduced by Rice and Tracey [13], namely

$$\mathbf{v} = \mathbf{v}^v + \mathbf{v}^S, \tag{9}$$

where $\mathbf{v}^v$ describes the expansion of the cavity while $\mathbf{v}^S$ is associated to shearing-related changes. Imposing the boundary conditions and matrix incompressibility, i.e.:

$$\mathbf{v}(\mathbf{x} = be_r) = \mathbf{D}\mathbf{x} \quad \text{and} \quad \operatorname{div}(\mathbf{v}) = 0,$$

where $\mathbf{x}$ is the Cartesian position vector that denotes the current position in the RVE and $\mathbf{e}_r$ is the radial unit vector, it follows that:

$$\mathbf{v}^v = \left(b^3/r^2\right) D_m \mathbf{e}_r \quad \text{and} \quad \mathbf{v}^S = \mathbf{D}'\mathbf{x} \tag{10}$$

where $r = \sqrt{x_1^2 + x_2^2 + x_3^2}$ is the radial coordinate, $D_m = (D_1 + D_2 + D_3)/3$ is the mean strain rate while $\mathbf{D}'$ is the deviator of $\mathbf{D}$.

It is worth noting that if the plastic flow in the matrix is governed by the von Mises criterion, the exact solution of the problem of a hollow sphere subjected to hydrostatic states (i.e. $\mathbf{D}' = 0$) is the term $\mathbf{v}^v = (b^3/r^2) D_m \mathbf{e}_r$ given by Eq. (10) (e.g., see [14]). Thus, for purely hydrostatic states (i.e. $D_1 = D_2 = D_3$), the above trial velocity is the only velocity field compatible with uniform strain rate boundary conditions.

In the Cartesian basis ($\mathbf{e}_1$, $\mathbf{e}_2$, $\mathbf{e}_3$) associated with the eigenvectors of $\mathbf{D}$ (see Eq. (8)), the local strain rate tensor $\mathbf{d} = (\nabla\mathbf{v} + \nabla\mathbf{v}^T)/2$ corresponding to the velocity field given by Eq. (10) is:

$$\begin{aligned}
d_{11} &= D_1' + b^3 D_m \frac{1 - 3x_1^2/(x_1^2 + x_2^2 + x_3^2)}{(x_1^2 + x_2^2 + x_3^2)^{3/2}} \\
d_{22} &= D_2' + b^3 D_m \frac{1 - 3x_2^2/(x_1^2 + x_2^2 + x_3^2)}{(x_1^2 + x_2^2 + x_3^2)^{3/2}} \\
d_{33} &= D_3' + b^3 D_m \frac{1 - 3x_3^2/(x_1^2 + x_2^2 + x_3^2)}{(x_1^2 + x_2^2 + x_3^2)^{3/2}} \\
d_{12} &= -\frac{3b^3 D_m x_1 x_2}{(x_1^2 + x_2^2 + x_3^2)^{3/2}}; \qquad d_{13} = -\frac{3b^3 D_m x_1 x_3}{(x_1^2 + x_2^2 + x_3^2)^{3/2}}; \qquad d_{23} = -\frac{3b^3 D_m x_2 x_3}{(x_1^2 + x_2^2 + x_3^2)^{3/2}}
\end{aligned} \tag{11}$$

where $D_i' = D_i - D_m, i = 1 \ldots 3$ are the eigenvalues of $\mathbf{D}'$.

Substitution of $\mathbf{d}$ given by Eq. (11) into Eq. (7), leads to the expression of the overall plastic dissipation associated to this velocity field, i.e.:

$$\Pi^+(\mathbf{D}, f) = \frac{\sigma_T}{V} \int_{\Omega} \sqrt{(2/3)\left(D_1'^2 + D_2'^2 + D_3'^2\right) + 4D_m^2 (b/r)^6 - 4D_m (b/r)^3 \left(D_1' x_1^2 + D_2' x_2^2 + D_3' x_3^2\right)} \mathrm{d}V, \tag{12}$$

with $V = 4\pi b^3/3$, Ω being the domain occupied by the matrix and the void.

Since the velocity $\mathbf{v}$ given by Eq. (10) is incompressible and compatible with homogeneous strain rate boundary conditions, Hill–Mandel lemma applies (see Eq. (4)–(5)) so $\Pi^+(\mathbf{D}, f)$ is an upper-bound estimate of the exact SRP of the porous solid given by Eq. (6). Note also that $\Pi^+(\mathbf{D}, \mathrm{f})$ depends on all principal values of the strain rate deviator $\mathbf{D}'$ and the mean strain rate, D_m. Equivalently, it can be expressed in terms of D_m and the invariants of $\mathbf{D}'$, namely $J_{2D} = \sqrt{(D_1'^2 + D_2'^2 + D_3'^2)/2}$, and $J_{3D} = D_1' D_2' D_3'$.

For general 3-D states, the integral expressing $\Pi^+(\mathbf{D}, \mathrm{f})$ (see Eq. (12)) cannot be estimated in closed form. However, for axisymmetric states, Cazacu et al. [8] have very recently shown that $\Pi^+(\mathbf{D}, \mathrm{f})$ can be calculated explicitly, without making any of the approximations generally considered in the literature. Note also that according to Eq. (12), $\Pi^+(\mathbf{D}, f)$ is an even function of $\mathbf{D}$ (i.e. it is invariant with respect to the transformation $(D_m, J_{2D}, J_{3D}) \to (-D_m, J_{2D}, -J_{3D})$), so only its expressions for the axisymmetric states corresponding to: ($D_m \geq 0$ and $D_1' = D_2' \geq 0$) and ($D_m \geq 0$ and $D_1' = D_2' \leq 0$)

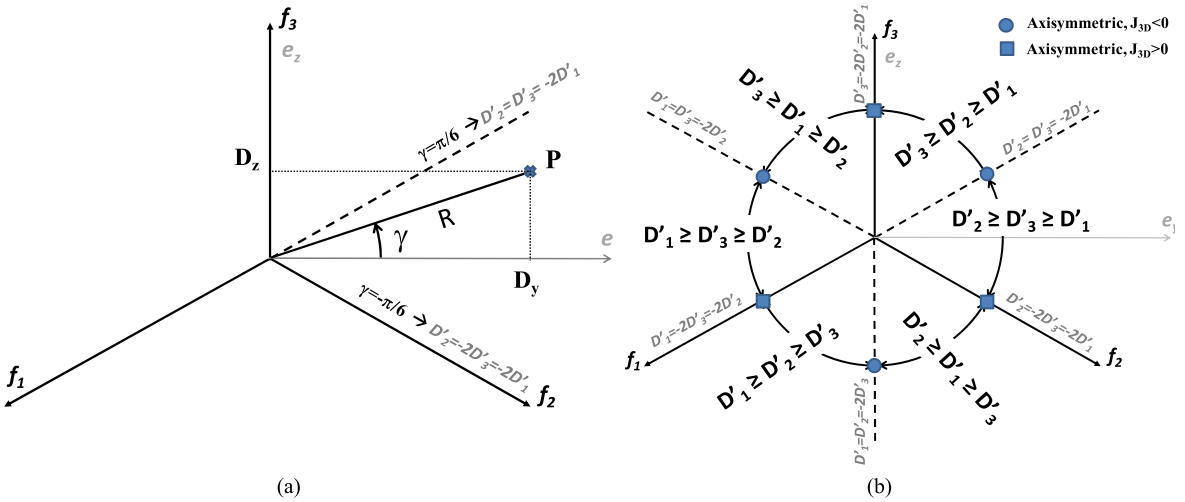

Fig. 1. (Color online.) (a) Definition of the polar-type coordinates (R, γ), representing any state P (D_1, D_2, D_3) belonging to the intersection of a strain rate potential (SRP) isosurface with any deviatoric plane (plane of normal the hydrostatic axis). (b) General symmetry properties of the cross-section of the strain rate potential of an isotropic material.

need to be calculated and will be given in the following. For all the other axisymmetric states, the respective expressions are obtained by symmetry (see also Fig. 1(b)).

Let us denote

$$u = \frac{D_{\mathrm{m}}}{\max\limits_{i=1..3}(|D'_i|)} \tag{13}$$

(i) For $D_{\mathrm{m}} \geq 0$ and $D'_1 = D'_2 \geq 0$:

$$\Pi^+(\mathbf{D}, f) = 2\sigma_{\mathrm{T}} D_{\mathrm{m}}\big[F(\sqrt{u/f}) - F(\sqrt{u})\big], \tag{14a}$$

where

$$F(z) = -2/\big(3z^2\big) + \frac{1}{3\sqrt{3}}\big[\tan^{-1}(2z+\sqrt{3}) - \tan^{-1}(2z-\sqrt{3})\big] + \ln\sqrt{z^4 - z^2 + 1} + \frac{3z^4 + 3z^2 - 1}{6\sqrt{3}z^3}\ln\left(\frac{z^2 + z\sqrt{3} + 1}{z^2 - z\sqrt{3} + 1}\right).$$

(ii) For $D_{\mathrm{m}} \geq 0$ and $D'_1 = D'_2 \leq 0$:

$$\begin{cases} \Pi^+(\mathbf{D}, f) = 2\sigma_{\mathrm{T}} D_{\mathrm{m}}\big[G(\sqrt{u/f}) - G(\sqrt{u})\big], & \forall u < f \\ \Pi^+(\mathbf{D}, f) = 2\sigma_{\mathrm{T}} D_{\mathrm{m}}\left[G(\sqrt{u}) + G(\sqrt{u/f}) + 2\ln(3) - \frac{2}{9}\frac{\pi}{\sqrt{3}}\right], & \forall f < u < 1 \\ \Pi^+(\mathbf{D}, f) = 2\sigma_{\mathrm{T}} D_{\mathrm{m}}\big[G(\sqrt{u}) - G(\sqrt{u/f})\big], & \forall u > 1 \end{cases} \tag{14b}$$

with:

$$G(z) = -2/\big(3z^2\big) - \frac{3z^4 - 3z^2 - 1}{3\sqrt{3}z^3}\tan^{-1}\left(\frac{z\sqrt{3}}{1 - z^2}\right) + \frac{1}{3\sqrt{3}}\left(\tan^{-1}\left(\frac{2z+1}{\sqrt{3}}\right) - \tan^{-1}\left(\frac{2z-1}{\sqrt{3}}\right)\right) - \ln\sqrt{z^4 + z^2 + 1}$$

For all other loadings, $\Pi^+(\mathbf{D}, f)$ cannot be calculated analytically and numerical integration methods need to be used. Isotropy dictates that $\Pi^+(\mathbf{D}, f)$ has three-fold symmetry with respect to the origin. Thus, it is sufficient to evaluate the integral expressing this SRP (Eq. (12)) only for states corresponding to: $D_2 \geq D_3 \geq D_1$ (see also Fig. 1(b)). If $D_2 \geq D_3 \geq D_1$, it follows that:

$$D'_1 = -\frac{R}{\sqrt{6}}(\sqrt{3}\cos\gamma + \sin\gamma)$$

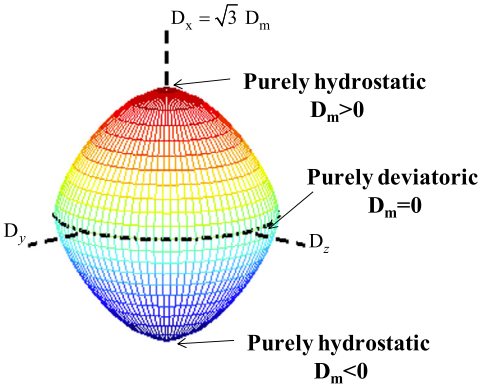

Fig. 2. (Color online.) The 3-D surface of a porous solid with a von Mises matrix according to Eq. (18) for both tensile mean strain rate ($D_m = \mathrm{tr}(\mathbf{D}) > 0$) and compressive ($D_m < 0$) states. Note that this convex surface contains all the points (D_m, R, γ) that produce the same plastic dissipation $\Pi^+(\mathbf{D}, f) = 9.21 \cdot 10^{-3}$ for the porous solid. Porosity: $f = 0.01$.

$$D'_2 = \frac{R}{\sqrt{6}}(\sqrt{3}\cos\gamma - \sin\gamma)$$
$$D'_3 = \frac{2R}{\sqrt{6}}\sin\gamma \tag{15}$$

with

$$R = \sqrt{D'^2_1 + D'^2_2 + D'^2_3} = \sqrt{2J_{2D}} \tag{16a}$$

and γ is the angle satisfying: $-\pi/6 \le \gamma \le \pi/6$ and whose sine is given by:

$$\sin 3\gamma = -\frac{27}{2}\cdot\frac{J_{3D}}{(J_{2D})^{3/2}} \tag{16b}$$

In particular, the sub-sector $-\pi/6 \le \gamma \le 0$ corresponds to states on the SRP for which ($D'_2 \ge 0, D'_3 \le 0, D'_1 \le 0$) so the third invariant $J_{3D} \ge 0$, while the sub-sector $0 \le \gamma \le \pi/6$ corresponds to states for which ($D'_2 \ge 0, D'_3 \ge 0, D'_1 \le 0$), so $J_{3D} \le 0$ (see also Fig. 1(b)). In this sub-sector, axisymmetric states correspond to either $\gamma = -\pi/6$ ($D'_1 = D'_3 < D'_2$) or $\gamma = \pi/6$ ($D'_2 = D'_3 > D'_1$). Note also that the angle γ, which is a measure of the combined effects of the second and third invariants, is related to the dimensionless parameter ν introduced by Drucker [15],

$$\nu = \frac{D'_{\mathrm{int}}}{D'_{\mathrm{min}} - D'_{\mathrm{max}}}, \tag{17}$$

where $D'_{\mathrm{min}} = \min(D'_1, D'_2, D'_3)$, $D'_{\mathrm{max}} = \max(D'_1, D'_2, D'_3)$ while D'_{int} is the intermediate principal value. Using Eqs. (15)–(16), the integral expression of the SRP can be put in the form:

$$\Pi^+(\mathbf{D}, f) = \frac{\sigma_T}{V}\int_{\Omega} 2\sigma_T\sqrt{\left(R^2/6\right) + D_m^2(b/r)^6 - 4RD_m(b/r)^3F\left(\gamma, x_i^2\right)/\left(r^2/\sqrt{6}\right)}\mathrm{d}V \tag{18}$$

with $F(\gamma, x_1^2, x_2^2, x_3^2) = \sqrt{3}(x_2^2 - x_1^2)\cos\gamma + (2x_3^2 - x_1^2 - x_2^2)\sin\gamma$.

Gaussian quadrature integration is used to evaluate the plastic dissipation $\Pi^+(\mathbf{D}, f)$ (Eq. (18)) for any 3-D loading. The hollow sphere domain is discretized with 125,000 hexahedral elementary volumes, with one integration point at the center. For axisymmetric loadings, the numerical estimate of $\Pi^+(\mathbf{D}, f)$ was compared to the exact result (i.e. Eq. (14)), differences being negligible (less than 10^{-7}).

As an example, in Fig. 2 is shown a 3-D isosurface of the von Mises porous solid (calculated using Eq. (18)) corresponding to a porosity $f = 1\%$ for both tensile ($D_m = \mathrm{tr}(\mathbf{D}) > 0$) and compressive ($D_m < 0$) states. Specifically, this convex surface contains all the points (D_m, R, γ) that produce the same plastic dissipation $\Pi^+(\mathbf{D}, f) = 9.21 \cdot 10^{-3}$ for the porous solid. First, let us note that the presence of voids induces a strong influence of the mean strain rate D_m on the plastic dissipation, the SRP being closed on the hydrostatic axis. Indeed, for purely hydrostatic states (i.e. $\mathbf{D} = D_m^H\mathbf{I}$) according to Eq. (14), $\Pi^+(\mathbf{D}, f) = 2\sigma_T|D_m^H|\ln f$. For $f = 1\%$ and plastic dissipation of $9.21 \cdot 10^{-3}$, this corresponds to: $D_m^H = \pm 1 \cdot 10^{-3}$ s^{-1}. Thus, the intersection of the isosurface with the planes $D_m = 1 \cdot 10^{-3}$ s^{-1} and $D_m = -1 \cdot 10^{-3}$ s^{-1}, respectively, are two points on the hydrostatic axis that are symmetric with respect to the origin (see also Fig. 2).

To fully assess the effects of all invariants of the strain rate, $\mathbf{D}$, on the plastic response of the porous solid, the cross-sections of the same 3-D isosurface with several deviatoric planes $D_m = \text{constant}$ are considered (see Fig. 3). For this

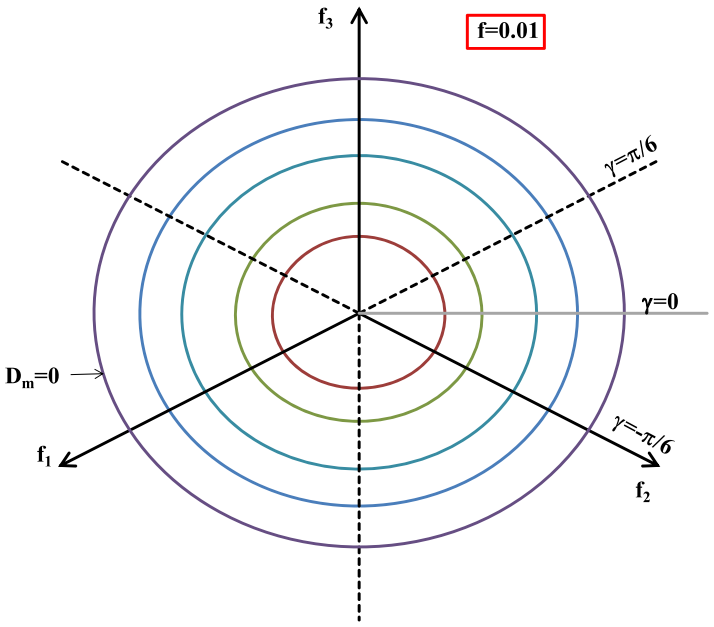

Fig. 3. (Color online.) Cross-sections of the 3-D isosurface of a porous von Mises material with several deviatoric planes $D_m = \text{constant}$: outer cross-section represents the intersection with the plane $D_m = 0$, while the inner cross-section corresponds to $D_m = 9 \cdot 10^{-4}\ s^{-1}$. Porosity: $f = 0.01$.

purpose, it is convenient to introduce a coordinate system of unit vectors ($\mathbf{e}_x$, $\mathbf{e}_y$, $\mathbf{e}_z$), which are related to the principal directions ($\mathbf{e}_1$, $\mathbf{e}_2$, $\mathbf{e}_3$) by the following relations:

$$\mathbf{e}_x = \frac{1}{\sqrt{3}}(\mathbf{e}_1 + \mathbf{e}_2 + \mathbf{e}_3), \qquad \mathbf{e}_y = -\frac{1}{\sqrt{2}}(\mathbf{e}_1 - \mathbf{e}_2), \qquad \mathbf{e}_z = \frac{1}{\sqrt{6}}(2\mathbf{e}_3 - \mathbf{e}_1 - \mathbf{e}_2). \tag{19}$$

Since the Ox-axis coincides with the hydrostatic axis, a plane that contains, say a point $P\ (D_1, D_2, D_3)$ on the isosurface and is parallel to the Oyz-plane also contains all the states belonging to the SRP with the same D_m (see Fig. 1). Thus, the intersection of the SRP with the deviatoric plane $D_m = \text{constant}$ is obtained by expressing the SRP in the (xyz) coordinates and then imposing $D_x = \text{constant}$. Let $\mathbf{f}_i$ be the projections of the eigenvectors $\mathbf{e}_i$, $i = 1 \ldots 3$ on a deviatoric plane. Note that the intersection of any surface $\Pi^+(\mathbf{D}, f) = \text{constant}$ with the plane $D_m = 0$, is a circle (see for example, Fig. 2). This is to be expected since states for which $D_m = 0$ correspond to purely deviatoric loadings for which the plastic dissipation of the porous solid coincides with that of the matrix (von Mises behavior). The cross-sections of the SRP with all the other deviatoric planes $D_m = c$ ($c \neq 0$) have three-fold symmetry with respect to the origin, and deviate slightly from a circle. This indicates that the third invariant $J_{3D} = D'_1 D'_2 D'_3$ affects the plastic response of the porous Mises material. It is also clearly seen that as D_m increases the response of the material becomes softer (the inner cross-section depicted in Fig. 3 corresponds to $D_m = 9 \cdot 10^{-4}\ s^{-1}$).

To assess the combined effects of J_{3D} and J_{2D} on the SRP of the porous von Mises material, the shapes of its cross-sections with deviatoric planes $D_m = c$ ($c \neq 0$) need to be determined. Due to isotropy, it is sufficient to study how the distance between the origin and any point on the cross-section evolves with γ in the sector $-\pi/6 \leq \gamma \leq \pi/6$. As already mentioned, in this sector, axisymmetric conditions correspond to $\gamma = -\pi/6$ ($D_1 = D_3 < D_2$) or $\gamma = \pi/6$ ($D_2 = D_3 < D_1$). As an example, in Fig. 4 is plotted $R(\gamma)$ (normalized by $R(\gamma = -\pi/6)$) for the cross-section corresponding to $D_m = 6 \cdot 10^{-4}\ s^{-1}$ and $D_m = 0$ (matrix behavior), respectively. Since the cross-section $D_m = 0$ is a circle, $R(\gamma) = \text{constant}$. As concerns the cross-section $D_m = 6 \cdot 10^{-4}\ s^{-1}$, note the influence of the third invariant J_{3D} (or γ) as evidenced by the deviation of $R(\gamma)/R(\gamma = -\pi/6)$ from a straight line. The noteworthy result is that the most pronounced difference is between the axisymmetric states, i.e. between $R(\gamma = -\pi/6)$ and $R(\gamma = \pi/6)$. This holds true irrespective of the level of D_m (see also Fig. 3). It follows that the most influence of the parameter γ (or J_{3D}) on the response of the porous solid (consequently its influence on void growth or void collapse) occurs for axisymmetric states. It is very worth noting that for the case of large positive and negative triaxialities, the same conclusions concerning the influence of the third invariant on void evolution were obtained in their seminal study by Rice and Tracey [13].

As pointed out in Cazacu et al. [8], a remarkable property of the exact plastic potentials (stress-based and strain rate based) of a porous solid with a von Mises matrix is their centro-symmetry. This property is preserved by $\Pi^+(\mathbf{D}, f)$. This means that for any porosity f : $\Pi^+(D_m, R, \gamma, f) = \Pi^+(-D_m, R, -\gamma, f)$, i.e. the surface is symmetric with respect to the origin (see also Eq. (18) and Fig. 2). More specifically, in Fig. 3 it is clearly seen that for a given D_m, in order to reach the same plastic dissipation in the porous solid, there should be a very specific dependence between the invariants of **D'**, i.e. between R and γ. Indeed, the analysis of the cross-sections shows that for $D_m > 0$, $R(\gamma)$ is a monotonically decreasing

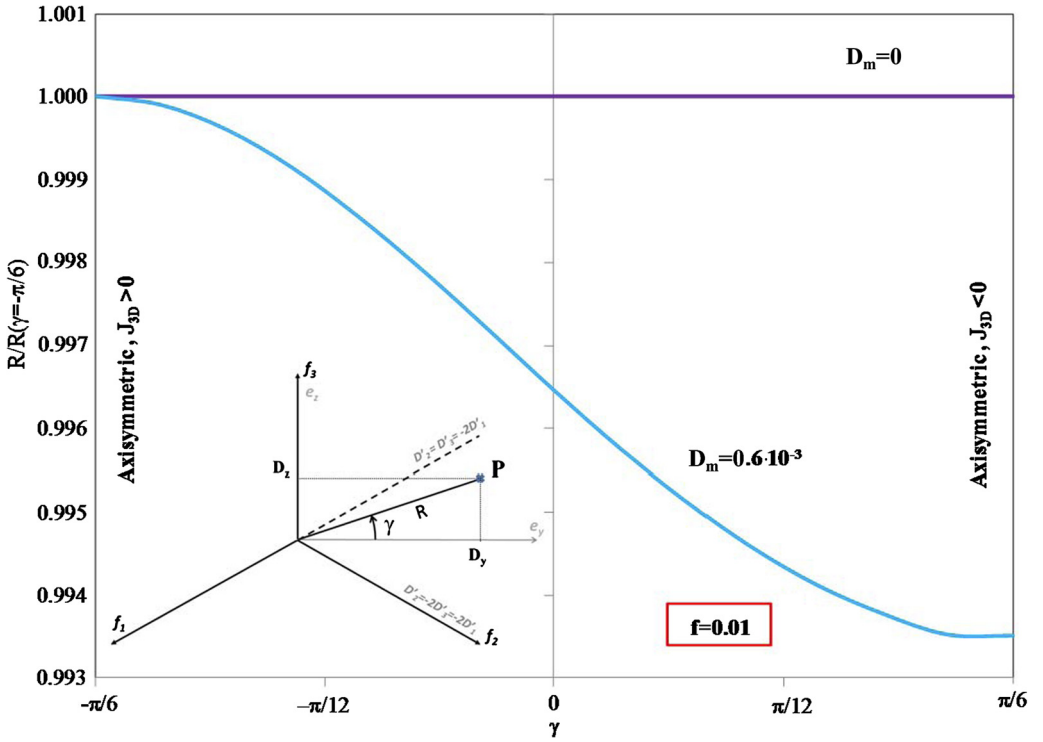

Fig. 4. (Color online.) Evolution of $R(\gamma)$ (normalized by $R = R(-\pi/6)$) for the cross-section of the surface of the porous Mises material with the deviatoric planes $D_m = 6 \cdot 10^{-4}$ s^{-1} and $D_m = 0$ (von Mises behavior), respectively. Initial porosity: $f = 0.01$. Note that the response depends on the third invariant as revealed by the very specific coupling between $R(=\sqrt{2J_{2D}})$ and γ (measure of J_{2D} and J_{3D}). Porosity $f = 0.01$.

function of γ (see Fig. 4). Due to the centro-symmetry of $\Pi^+(\mathbf{D}, f)$ for $D_m < 0$, $R(\gamma)$ must be a monotonically increasing function of γ. A function that has these properties and coincides with the exact values of $R(\gamma)$ for axisymmetric states is considered:

$$R(\gamma) = \frac{R_- + R_+}{2} + \frac{R_- - R_+}{2}\left(\frac{\sinh(\gamma) - \gamma\cosh(\pi/6)}{-\sinh(\pi/6) + \frac{\pi}{6}\cosh(\pi/6)}\right), \tag{20}$$

where R_- and R_+ are the exact values of the SRP corresponding to axisymmetric loadings at $\gamma = -\pi/6$ and $\gamma = \pi/6$, respectively, which are calculated using Eq. (14). Since any state $\mathbf{D}$ belonging to the isosurface $\Pi^+(\mathbf{D}, f) = k$, with constant k fully defined by $(D_m, R(\gamma), \gamma)$, for any given (D_m, γ), first we need to solve:

$$\begin{aligned} &\Pi^+\left(D_m, R_-, -\frac{\pi}{6}, f\right) = k \\ &\Pi^+\left(D_m, R_+, \frac{\pi}{6}, f\right) = k \end{aligned} \tag{21}$$

to find R_- and R_+ associated with the given D_m and then use Eq. (20) to determine $R(\gamma)$.

In the above equation, $\Pi^+(D_m, R_-, -\frac{\pi}{6}, f)$ is calculated using the analytic expression of the plastic dissipation for the axisymmetric case $D_m > 0$ and $J_{3D} > 0$ (Eq. (14b)), while $\Pi^+(D_m, R_+, \frac{\pi}{6}, f)$ corresponds to the axisymmetric case $D_m > 0$ and $J_{3D} < 0$ (Eq. (14a)).

Comparison between the evolution of R(γ) (normalized by $R(-\pi/6)$) according to Eq. (20) and the numerical values obtained by estimating numerically the integral of Eq. (18) (symbols) is shown in Fig. 5 for the cross-sections of the isosurface $\Pi^+(\mathbf{D}, f) = 9.21 \cdot 10^{-3}$ corresponding to a porosity $f = 0.01$ with the deviatoric planes $D_m = 4 \cdot 10^{-4}$ s^{-1} and $D_m = 6 \cdot 10^{-4}$ s^{-1}, respectively. The shapes in the sector $-\pi/6 \le \gamma \le \pi/6$ of the cross-sections of the proposed analytical SRP (Eq. (20)) with several deviatoric planes $D_m =$ constant and the numerical points (symbols) are shown in Fig. 6. Note that the proposed function is a very good approximation for all values of $D_m > 0$ considered.

2.2. Comparison between the proposed SRP and Gurson's SRP

As already mentioned, the most widely used plastic potential for isotropic porous solids containing randomly distributed spherical voids was proposed by Gurson [1]. This yield criterion was derived by conducting limit analysis of a hollow sphere

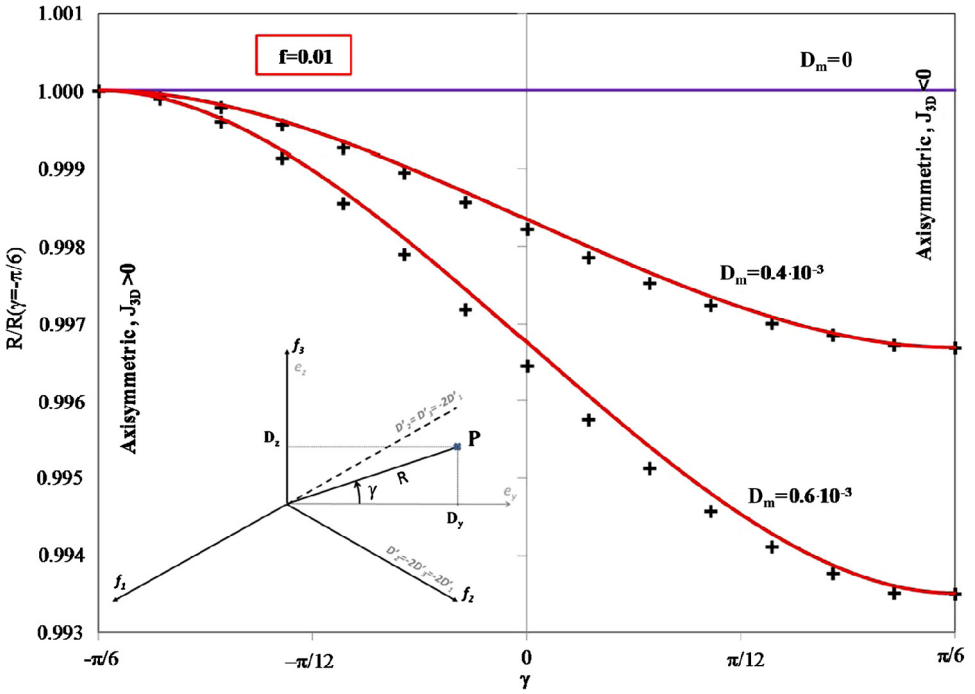

Fig. 5. (Color online.) Comparison between the evolution of $R(\gamma)$ (normalized by $R = R(-\pi/6)$) according to Eq. (20) and the numerical values (symbols) for the cross-section of the surface of the porous Mises material with the deviatoric planes: $D_{\mathrm{m}} = 6 \cdot 10^{-4}\ \mathrm{s}^{-1}$, $D_{\mathrm{m}} = 4 \cdot 10^{-4}\ \mathrm{s}^{-1}$, and $D_{\mathrm{m}} = 0$, respectively. Porosity: $f = 0.01$.

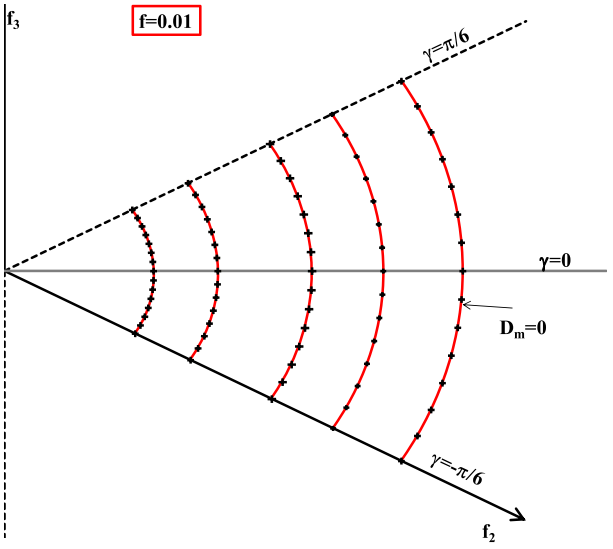

Fig. 6. (Color online.) Cross-sections of the new 3-D strain rate potential corresponding to a fixed value of the plastic dissipation $9.21 \cdot 10^{-3}$ with several deviatoric planes $D_{\mathrm{m}} =$ constant: outer cross-section represents the intersection with the plane $D_{\mathrm{m}} = 0$ while the inner cross-section corresponds to $D_{\mathrm{m}} = 9 \cdot 10^{-4}\ \mathrm{s}^{-1}$. Numerical points are represented by symbols. Porosity: $f = 0.01$.

made of a rigid-plastic material obeying the von Mises yield criterion using the trial velocity field deduced by Rice and Tracey [13] (see Eq. (10)). In his analysis, Gurson [12,1] assumed that the coupled effects between the mean strain rate D_{m} and **D**' (i.e. the cross-term $D_{\mathrm{m}}(b/r)^3(D'_1x_1^2 + D'_2x_2^2 + D'_3x_3^2)$ in the expression of $\Pi^+(\mathbf{D}, f)$ given by Eq. (12)) can be neglected and obtained the following expression for the strain rate potential:

$$\Pi_{\mathrm{Gurson}}(\mathbf{D}, f) = 2|D_{\mathrm{m}}|\left[\frac{\sqrt{1+6D_{\mathrm{m}}^2/R^2} - \sqrt{f^2+6D_{\mathrm{m}}^2/R^2}}{(D_{\mathrm{m}}/R)\sqrt{6}} + \ln\left(\frac{1}{f} \times \frac{(D_{\mathrm{m}}/R)\sqrt{6} + \sqrt{f^2+6D_{\mathrm{m}}^2/R^2}}{(D_{\mathrm{m}}/R)\sqrt{6} + \sqrt{1+6D_{\mathrm{m}}^2/R^2}}\right)\right] \tag{22}$$

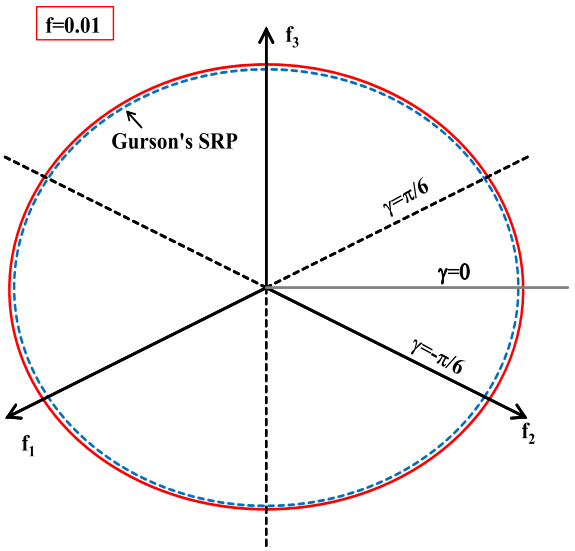

Fig. 7. (Color online.) Comparison between the cross-sections of the new 3-D strain rate potential (interrupted line; Eq. (20)–(21)) and that of the strain rate potential dual to Gurson's [1] (solid line) corresponding to the same level of plastic energy $9.21 \cdot 10^{-3}$. The cross-section correspond to $D_m = 6 \cdot 10^{-4}$ s^{-1}. Note that Gurson's SRP is more dissipative than the new model. Porosity: $f = 0.01$.

Note that $\Pi_{\text{Gurson}}(\mathbf{D}, f)$ is the work-conjugate of the classic stress-based potential of Gurson [1] given by Eq. (1). Gurson's SRP given by Eq. (22) does not involve any dependence on the third invariant J_{3D} (or γ). Therefore, irrespective of D_m or of the porosity level, the cross-section of $\Pi_{\text{Gurson}}(\mathbf{D}, f)$ with any deviatoric plane $D_m = c$ ($c =$ constant) is always a circle, i.e. $R =$ constant (see also Fig. 7). Gurson's SRP involves only dependence of D_m and J_{2D} (or R) and displays stronger symmetry properties, being also invariant to the transformation $(D_m, R) \to (-D_m, -R)$. In other words, the dilatational response according to Gurson's SRP is insensitive to the sign of the mean strain rate D_m.

On the other hand, the proposed analytical SRP (Eqs. (20)–(21)) depends on all three invariants. It has the following properties:

- it coincides with the exact SRP for axisymmetric states,
- since $R(\gamma)$ given by Eq. (20) is an odd function and relies on the exact analytical values for axisymmetric states, it satisfies automatically the centro-symmetry requirement, i.e. it is invariant to the transformation $(D_m, R, \gamma) \to (-D_m, R, -\gamma)$,
- the derivative of $R(\gamma)$ with respect to γ is null for axisymmetric loadings (see Eq. (20)),
- the SRP displays three-fold symmetry with respect to the origin.

Thus, the proposed analytic SRP (Eqs. (20)–(21)) preserves all the key features of the exact SRP. To further illustrate the specific differences between the proposed SRP and Gurson's in Fig. 7 are shown the cross-sections with the deviatoric plane $D_m = 6 \cdot 10^{-4}$ s^{-1} of the respective isosurfaces corresponding to the same value of the plastic dissipation ($9.21 \cdot 10^{-3}$) and the same void volume fraction ($f = 1\%$). Since Gurson's SRP was obtained by truncating the overall plastic dissipation (see Eq. (21)), it is necessarily interior to the proposed SRP. This means that Gurson's SRP is more dissipative, i.e. in order to reach the same value of the plastic dissipation, the norm of the loading, $R(\gamma)$, for Gurson's SRP is lower than that for the proposed SRP (Eq. (20)). Only for purely hydrostatic loading ($\mathbf{D}' = 0$), and purely deviatoric states ($D_m = 0$), the new SRP coincides with the proposed SRP.

3. New analytic stress-based potential for a porous solid with a von Mises matrix

Since the cavities are spherical and randomly distributed in an isotropic matrix, the porous von Mises material is isotropic. It follows that the principal directions of the overall stress at yielding, $\boldsymbol{\Sigma}$, and that of the macroscopic strain rate tensor $\mathbf{D}$ coincide. Thus, at yielding (see Eq. (6))

$$\Sigma_i = \frac{\partial \Pi^+(\mathbf{D}, f)}{\partial D_i}, \quad i = 1 \ldots 3 \tag{23}$$

where Σ_i are the principal values of the macroscopic stress tensor and $\Pi^+(\mathbf{D}, f)$ is given by Eq. (18). For axisymmetric states, the expressions of $\Pi^+(\mathbf{D}, f)$ are given by Eq. (14). By further substituting Eq. (14) into Eq. (23), the parametric representation of the yield surface is obtained (for more details the reader is referred to Cazacu et al. [8]). Its expressions are:

(a) for $J_3^{\Sigma} \le 0$, $\Sigma_m \ge 0$, and any value of u (see definition of u given by Eq. (13)):

$$\begin{cases} \dfrac{\Sigma_m}{\sigma_T} = \dfrac{1}{9}\dfrac{1-f}{u} + \dfrac{1}{3}\ln\left(\dfrac{u^2-uf+f^2}{u^2-u+1}\dfrac{1}{f^2}\right) + \dfrac{1}{18\sqrt{3}}\ln\left(\dfrac{u+\sqrt{3uf}+f}{u-\sqrt{3uf}+f}\right)\left(\dfrac{9u^2+3uf+f^2}{u^{3/2}\sqrt{f}}\right) \\ \qquad - \dfrac{1}{18\sqrt{3}}\ln\left(\dfrac{u+\sqrt{3u}+1}{u-\sqrt{3u}+1}\right)\left(\dfrac{9u^2+3u+1}{u^{3/2}}\right) + \dfrac{2}{18\sqrt{3}}\left(\tan^{-1}\left(2\sqrt{\dfrac{u}{f}}+\sqrt{3}\right)\right. \\ \qquad \left. - \tan^{-1}\left(2\sqrt{\dfrac{u}{f}}-\sqrt{3}\right)\right) - \dfrac{2}{18\sqrt{3}}\left(\tan^{-1}(2\sqrt{u}+\sqrt{3}) - \tan^{-1}(2\sqrt{u}-\sqrt{3})\right) \\ \dfrac{\Sigma_e}{\sigma_T} = \dfrac{1-f}{2} + \dfrac{1}{4\sqrt{3u}}\left[(u^2-u+1)\ln\left(\dfrac{u+\sqrt{3u}+1}{u-\sqrt{3u}+1}\right) - \dfrac{(u^2-uf+f^2)}{\sqrt{f}}\ln\left(\dfrac{u+\sqrt{3uf}+f}{u-\sqrt{3uf}+f}\right)\right] \end{cases} \tag{24a}$$

(b) for $J_3^{\Sigma} \le 0$ and $\Sigma_m \le 0$:

(b1) if $u \le f$:

$$\begin{cases} \dfrac{\Sigma_m}{\sigma_T} = \dfrac{f-1}{9u} + \dfrac{1}{3}\ln\left(\dfrac{u^2+uf+f^2}{(u^2+1+u)f^2}\right) - \dfrac{1}{9\sqrt{3fu^3}}\left(\left(9u^2-3uf+f^2\right)\tan^{-1}\left(\dfrac{\sqrt{3uf}}{f-u}\right)\right. \\ \qquad \left. - \left(9u^2-3u+1\right)\tan^{-1}\left(\dfrac{\sqrt{3u}}{1-u}\right)\right) - \dfrac{2}{9\sqrt{3}}\left(\tan^{-1}\left(\dfrac{2\sqrt{u}+\sqrt{f}}{\sqrt{3f}}\right) + \tan^{-1}\left(\dfrac{2\sqrt{u}-1}{\sqrt{3}}\right)\right. \\ \qquad \left. - \tan^{-1}\left(\dfrac{2\sqrt{u}-\sqrt{f}}{\sqrt{3f}}\right) - \tan^{-1}\left(\dfrac{2\sqrt{u}+1}{\sqrt{3}}\right)\right) \\ \dfrac{\Sigma_e}{\sigma_T} = \dfrac{f|u-1|-|u-f|}{2u} - \dfrac{1}{2\sqrt{3}}\left[\dfrac{(u^2+uf+f^2)\tan^{-1}\left(\frac{\sqrt{3uf}}{|f-u|}\right)}{\sqrt{uf}} - \dfrac{(1+u+u^2)\tan^{-1}\left(\frac{\sqrt{3u}}{|1-u|}\right)}{\sqrt{u}}\right] \end{cases} \tag{24b}$$

(b2) if $f < u < 1$:

$$\begin{cases} \dfrac{\Sigma_m}{\sigma_T} = \dfrac{2}{3}\ln(3) - \dfrac{2}{18}\dfrac{\pi}{\sqrt{3}} - \dfrac{1+f-2u}{9u} - \dfrac{1}{3}\ln\left(\dfrac{(u^2+1+u)(u^2+uf+f^2)}{f^2}\right) \\ \qquad + \dfrac{1}{9\sqrt{3u^3}}\left(\left(9u^2-3u+1\right)\arctan\left(\dfrac{\sqrt{3u}}{1-u}\right) - \left(9u^2-3uf+f^2\right)\arctan\left(\dfrac{\sqrt{3fu}}{f-u}\right)\right) \\ \qquad + \dfrac{2}{9\sqrt{3}}\left(\arctan\left(\dfrac{2\sqrt{u}+\sqrt{f}}{\sqrt{3f}}\right) - \arctan\left(\dfrac{2\sqrt{u}-\sqrt{f}}{\sqrt{3f}}\right) + \arctan\left(\dfrac{2\sqrt{u}+1}{\sqrt{3}}\right)\right. \\ \qquad \left. - \arctan\left(\dfrac{2\sqrt{u}-1}{\sqrt{3}}\right)\right) \\ \dfrac{\Sigma_e}{\sigma_T} = \dfrac{1}{2}(1+f) - u + \dfrac{1}{2\sqrt{3u}}\left(\dfrac{(u^2+uf+f^2)}{\sqrt{f}}\tan^{-1}\left(\dfrac{\sqrt{3uf}}{f-u}\right) + \left(u^2+1+u\right)\tan^{-1}\left(\dfrac{\sqrt{3u}}{1-u}\right)\right) \end{cases} \tag{24c}$$

(b3) if $u \ge 1$:

$$\begin{cases} \dfrac{\Sigma_m}{\sigma_T} = \dfrac{1-f}{9u} - \dfrac{1}{3}\ln\left(\dfrac{u^2+uf+f^2}{(u^2+1+u)f^2}\right) + \dfrac{1}{9\sqrt{3fu^3}}\left(\left(9u^2-3uf+f^2\right)\tan^{-1}\left(\dfrac{\sqrt{3uf}}{f-u}\right)\right. \\ \qquad \left. - \left(9u^2-3u+1\right)\tan^{-1}\left(\dfrac{\sqrt{3u}}{1-u}\right)\right) + \dfrac{2}{9\sqrt{3}}\left(\tan^{-1}\left(\dfrac{2\sqrt{u}+\sqrt{f}}{\sqrt{3f}}\right) + \tan^{-1}\left(\dfrac{2\sqrt{u}-1}{\sqrt{3}}\right)\right. \\ \qquad \left. - \tan^{-1}\left(\dfrac{2\sqrt{u}-\sqrt{f}}{\sqrt{3f}}\right) - \tan^{-1}\left(\dfrac{2\sqrt{u}+1}{\sqrt{3}}\right)\right) \\ \dfrac{\Sigma_e}{\sigma_T} = \dfrac{f|u-1|-|u-f|}{2u} - \dfrac{1}{2\sqrt{3}}\left[\dfrac{(u^2+uf+f^2)\tan^{-1}\left(\frac{\sqrt{3uf}}{|f-u|}\right)}{\sqrt{uf}} - \dfrac{(1+u+u^2)\tan^{-1}\left(\frac{\sqrt{3u}}{|1-u|}\right)}{\sqrt{u}}\right] \end{cases} \tag{24d}$$

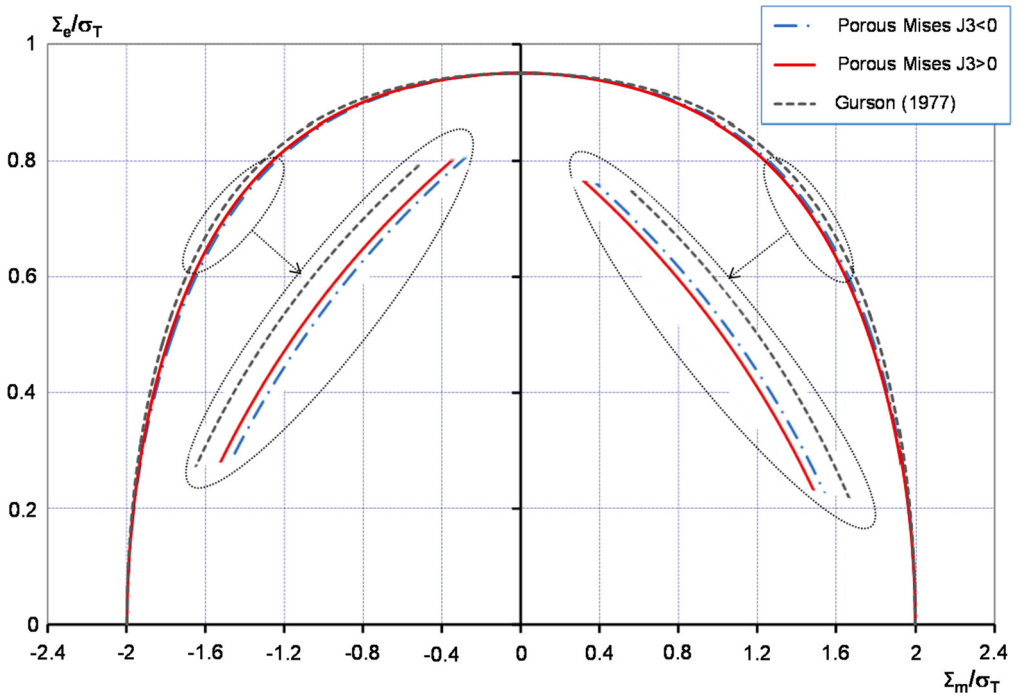

Fig. 8. (Color online.) Yield surface of the porous solid according to Cazacu et al. [8] criterion for axisymmetric stress states for loadings such that $J_3^{\Sigma} \leq 0$ and $J_3^{\Sigma} \geq 0$, respectively, in comparison with Gurson's [1] for the same porosity ($f = 0.05$).

The yield surface being centro-symmetric, the parametric representation of the yield locus corresponding to $J_3^{\Sigma} \geq 0$ can be easily obtained from Eq. (24):

(c) For $J_3^{\Sigma} \geq 0$ and $\Sigma_m \geq 0$:

$$\begin{cases} \dfrac{\Sigma_m}{\sigma_T} = -\dfrac{\Sigma_m}{\sigma_T}\Big|_{J_3^{\Sigma}\leq 0,\, \Sigma_m \leq 0} \\ \dfrac{\Sigma_e}{\sigma_T} = \dfrac{\Sigma_e}{\sigma_T}\Big|_{J_3^{\Sigma}\leq 0,\, \Sigma_m \leq 0} \end{cases} \tag{25a}$$

where the right-hand expressions are given by Eqs. (24a)–(24d).

(d) For $J_3^{\Sigma} \geq 0$ and $\Sigma_m \leq 0$:

$$\begin{cases} \dfrac{\Sigma_m}{\sigma_T} = -\dfrac{\Sigma_m}{\sigma_T}\Big|_{J_3^{\Sigma}\leq 0,\, \Sigma_m \geq 0} \\ \dfrac{\Sigma_e}{\sigma_T} = \dfrac{\Sigma_e}{\sigma_T}\Big|_{J_3^{\Sigma}\leq 0,\, \Sigma_m \geq 0} \end{cases} \tag{25b}$$

where the right-hand expressions are given by Eq. (24a).

It can be easily seen that for purely hydrostatic loading ($u \to \infty$ in Eq. (24a)), we obtain: $|\Sigma_m| = \frac{2}{3}\sigma_T \ln f$ and $\Sigma_e = 0$; and for purely deviatoric loading ($u \to 0$), $\Sigma_m = 0$, and $\Sigma_e = \sigma_T(1 - f)$, irrespective of the sign of J_3^{Σ}.

In Fig. 8 are presented the yield curves according to the criterion given by Eqs. (24)–(25) corresponding to $J_3^{\Sigma} \geq 0$ and $J_3^{\Sigma} \leq 0$, respectively, and the Gurson yield surface (see Eq. (1)) for a porosity $f = 0.05$. Note that for axisymmetric loading, $\boldsymbol{\Sigma} = \Sigma_{11}(\mathbf{e}_1 \otimes \mathbf{e}_1 + \mathbf{e}_2 \otimes \mathbf{e}_2) + \Sigma_{33}(\mathbf{e}_3 \otimes \mathbf{e}_3)$, the von Mises equivalent stress is $\Sigma_e = |\Sigma_{11} - \Sigma_{33}|$, the mean stress is $\Sigma_m = (2\Sigma_{11} + \Sigma_{33})/3$, and the third invariant of the stress deviator is $J_3^{\Sigma} = -\frac{2}{27}(\Sigma_{11} - \Sigma_{33})^3$, so $J_3^{\Sigma} \leq 0$ corresponds to stress states for which $\Sigma_{11} \geq \Sigma_{33}$, while $J_3^{\Sigma} \geq 0$ corresponds to stress states for which $\Sigma_{11} \leq \Sigma_{33}$. Note that for $\Sigma_m \geq 0$, the response is softer for $J_3^{\Sigma} \geq 0$ than for $J_3^{\Sigma} \leq 0$ (see also the different zooms of the yield curves shown in Fig. 8). For purely deviatoric loading, the response is the same, and the effect of J_3^{Σ} becomes noticeable with increasing triaxiality. For triaxialities approaching infinity, the effect of J_3^{Σ} starts to decrease, and both yield curves coincide at the purely hydrostatic point. It is clearly seen that Gurson's criterion (Eq. (1)) is an upper bound of the criterion given by Eq. (24).

For all other loadings, $\Pi^+(\mathbf{D}, f)$ (see Eq. (12)) cannot be calculated analytically. Furthermore substitution of Eq. (12) into Eq. (23) and further evaluation of these integrals numerically leads to:

$$\Sigma_i = \frac{2\sigma_T}{3V}\int\limits_{\Omega} \frac{D'_i + 2D_m b^6/r^6 - b^3(D'_1x_1^2 + D'_2x_2^2 + D'_3x_3^2)/r^5 - D_m b^3(3x_1^2 - r^2)/r^5}{\sqrt{D_e^2 + 4D_m^2 b^6/r^6 - 4D_m(D'_1x_1^2 + D'_2x_2^2 + D'_3x_3^2)b^3/r^5}}\,dV \tag{26}$$

One of the objectives of this study is to develop an approximate 3-D stress-based potential that preserves the key properties of the exact one and reduces to the exact yield criterion for axisymmetric states. The stress potential that it is proposed relies on the analysis of the couplings between all invariants of the strain rate of deformation, $\mathbf{D}$, on the plastic dissipation $\Pi^+(\mathbf{D}, f)$ that were revealed by the 3-D numerical calculations presented in the previous section.

First, note that the exact stress-based plastic potential of the porous material is the work conjugate (exact dual) of the overall plastic potential $\Pi^+(\mathbf{D}, f)$ (see Eq. (18)). Therefore, the stress-based plastic potential of the porous von Mises material should have the following remarkable properties:

(i) it should depend on all stress invariants,
(ii) it ought to be centro-symmetric, i.e. invariant to the transformation: $(\Sigma_m, \Sigma_e, J_3^\Sigma) \to (-\Sigma_m, \Sigma_e, -J_3^\Sigma)$,
(iii) it should be an even function in stresses,
(iv) the most influence of the third invariant of the stress deviator should be for axisymmetric states.

The stress-potential being isotropic, it is sufficient to provide its expression in the sector $\Sigma_2 \geq \Sigma_3 \geq \Sigma_1$ (see also Fig. 1(b)). If $\Sigma_2 \geq \Sigma_3 \geq \Sigma_1$, it follows that:

$$\begin{aligned}
\Sigma'_1 &= -\frac{\tilde{R}}{\sqrt{6}}(\sqrt{3}\cos\theta + \sin\theta)\\
\Sigma'_2 &= \frac{\tilde{R}}{\sqrt{6}}(\sqrt{3}\cos\theta - \sin\theta)\\
\Sigma'_3 &= \frac{2\tilde{R}}{\sqrt{6}}\sin\theta
\end{aligned} \tag{27}$$

with

$$\tilde{R} = \sqrt{\Sigma_1'^2 + \Sigma_2'^2 + \Sigma_3'^2} = \sqrt{(2/3)\Sigma_e}, \tag{28a}$$

and θ is the angle satisfying: $-\pi/6 \leq \theta \leq \pi/6$ and whose sine is given by:

$$\sin 3\theta = -\frac{27}{2}\cdot\frac{J_3^\Sigma}{(J_2^\Sigma)^{3/2}}. \tag{28b}$$

In particular, the sub-sector $-\pi/6 \leq \theta \leq 0$ corresponds to states on the surface for which ($\Sigma'_2 \geq 0$, $\Sigma'_3 \leq 0$, $\Sigma'_1 \leq 0$), so the third invariant $J_3^\Sigma \geq 0$, while the sub-sector $0 \leq \theta \leq \pi/6$ corresponds to states for which ($\Sigma'_2 \geq 0$, $\Sigma'_3 \geq 0$, $\Sigma'_1 \leq 0$), so $J_3^\Sigma \leq 0$. In this sector, axisymmetric states correspond to either $\theta = -\pi/6$ ($\Sigma'_1 = \Sigma'_3 < \Sigma'_2$) or $\theta = \pi/6$ ($\Sigma'_2 = \Sigma'_3 > \Sigma'_1$).

To describe the variation of $\tilde{R} = \sqrt{(2/3)\Sigma_e}$ with the angle θ (measure of the combined influence of Σ_e and J_3^Σ), the following approximation is considered:

$$\tilde{R}(\theta) = (\tilde{R}_+ + \tilde{R}_-)/2 + \frac{(\tilde{R}_- - \tilde{R}_+)}{2}\left(\frac{\sinh(\theta) - \theta\cosh(\pi/6)}{-\sinh(\pi/6) + \frac{\pi}{6}\cosh(\pi/6)}\right) \tag{29}$$

where $\tilde{R}_-$ and $\tilde{R}_+$ are the exact values corresponding to axisymmetric loadings at $\gamma = -\pi/6$ and $\gamma = \pi/6$, respectively (calculated using Eq. (25)).

As an example, in Fig. 9 is shown the 3-D yield surface given by Eq. (28) corresponding to a porosity $f = 1\%$ for both tensile ($\Sigma_m > 0$) and compressive ($\Sigma_m < 0$) states. Specifically, this convex surface contains all the stress points corresponding to the same plastic dissipation for the porous solid. First, let us note that the presence of voids induces a strong influence of the mean stress Σ_m on yielding. The yield surface is closed on the hydrostatic axis. Indeed, for purely hydrostatic states (i.e. $\Sigma = \Sigma_m^H\mathbf{I}$) according to Eq. (23), yielding occurs for: $|\Sigma_m^H| = \frac{2}{3}\sigma_T \ln f$. For purely deviatoric loadings (i.e. loadings at $\Sigma_m = 0$): $\Sigma_e = \sigma_T(1-f)$. Fig. 10 shows the cross-sections of the new 3-D yield criterion given by Eq. (29) with several deviatoric planes $\Sigma_m =$ constant. Note that irrespective of the value of Σ_m, the cross-sections slightly deviate from circles, the most influence of the third invariant of the stress deviator occurs for axisymmetric conditions. Also, with increasing Σ_m, the influence of the third invariant (or γ) is increasing.

Since the proposed dependence of $\tilde{R}$ with θ relies on the exact values for axisymmetric loadings and it is an odd function, the key properties of the exact stress-based plastic potential are preserved. Most importantly, the yield surface according to the proposed criterion is centro-symmetric. To illustrate this noteworthy property in Fig. 11 are shown the cross-sections

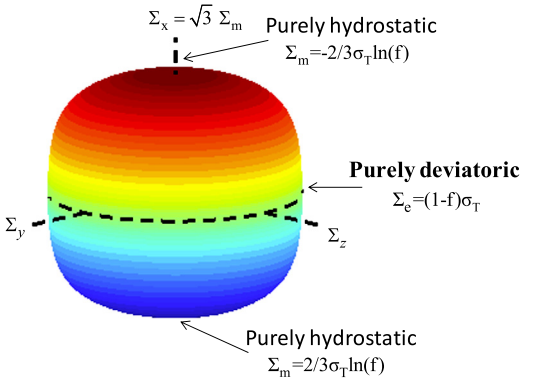

Fig. 9. (Color online.) The 3-D stress surface for a porous solid with a von Mises matrix according to the new model (Eq. (29)) for both tensile and compressive states. Porosity: $f = 0.01$.

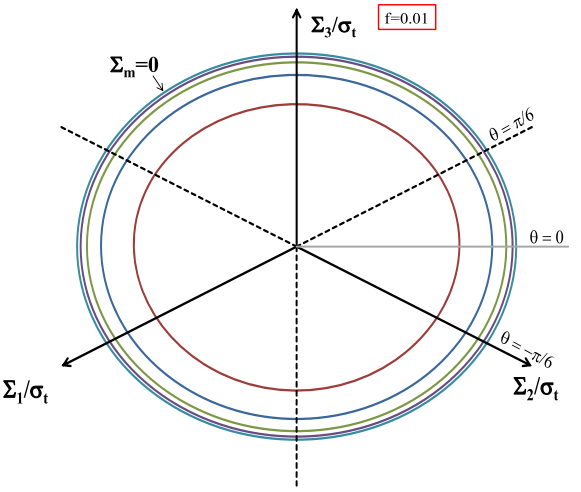

Fig. 10. (Color online.) Cross-sections of the new 3-D yield surface (Eq. (29)) of a porous von Mises material with several deviatoric planes $\Sigma_m = \text{constant}$: outer cross-section represents the intersection with the plane $\Sigma_m/\sigma_T = 0$ while the inner cross-section corresponds to $\Sigma_m/\sigma_T = 2.5$. Porosity: $f = 0.01$.

of the yield surface according to Eq. (29) corresponding to a porosity $f = 0.01$ with a deviatoric plane corresponding to a positive mean stress ($\Sigma_m/\sigma_T = 2$, interrupted line) and a compressive mean stress ($\Sigma_m/\sigma_T = -2$, solid line), respectively. The symmetry of the respective cross-sections with respect to the origin is clearly seen. For example, for loadings corresponding to $J_3^{\Sigma} \geq 0$ (i.e. $-\pi/6 \leq \theta \leq 0$) to produce the same plastic dissipation, $\tilde{R}(\theta)$ (or $\sqrt{(2/3)\Sigma_e}$) at yielding must be lower for compressive states ($\Sigma_m < 0$ – interrupted line) than for tensile states ($\Sigma_m > 0$ – solid line). The reverse holds true for loadings corresponding to $J_3^{\Sigma} \leq 0$ ($0 \leq \theta \leq \pi/6$).

Note also the clear departure from Gurson's stress criterion (Eq. (1)). As an example, in Fig. 12(a)–(b) are shown the cross-sections of the new yield criterion (Eq. (29)) and that of Gurson's (Eq. (1)) with the deviatoric planes $\Sigma_m/\sigma_T = 1.5$ and $\Sigma_m/\sigma_T = 2$, respectively for a void volume fraction $f = 1\%$. Gurson's criterion (interrupted line) is an upper bound to the new criterion, the correction brought to Gurson's criterion becoming more significant with increasing Σ_m. This important point is further illustrated in Fig. 13, which shows the differences between the two criteria as a function of γ for several cross-section $\Sigma_m/\sigma_T = \text{constant}$. It is also worth noting that the most important difference between Gurson's [1] criterion and the new criterion is always for axisymmetric conditions.

To further illustrate the specific couplings between all stress invariants, in Fig. 14 are shown the intersection of the new yield surface with planes $\theta = \text{constant}$ (i.e. $\theta = -\pi/6$, $\theta = 0$, $\theta = \pi/12$ and $\theta = \pi/6$, respectively) for tensile states ($\Sigma_m \geq 0$). Note that according to the new criterion, the influence of θ, which is a measure of the couplings between J_3^{Σ} and Σ_e (or J_2^{Σ}) is very small for low stress triaxialities, but there is an increasing influence of θ with increasing stress triaxiality (see also Figs. 14(a)–14(b)); for stress states corresponding to stress triaxialities $T = (\Sigma_m/\Sigma_e)$ approaching infinity (i.e. purely hydrostatic states), the effect of θ starts to decrease, and the yield curves for the different θ coincide at the purely hydrostatic point ($\Sigma_e = 0$) (see Fig. 14(c)). Irrespective of the level of the stress triaxiality T, the softest response is for axisymmetric loadings corresponding to $\theta = -\pi/6$ ($J_{3\Sigma} > 0$) while the hardest response is for $\theta = \pi/6$ ($J_{3\Sigma} < 0$). Note that due to the centro-symmetry of the yield surface, for compressive mean stress the softest response is for axisymmetric loadings corresponding to $\theta = -\pi/6$ ($J_{3\Sigma} > 0$), while the hardest response is for $\theta = \pi/6$ ($J_{3\Sigma} < 0$) (see Fig. 15).

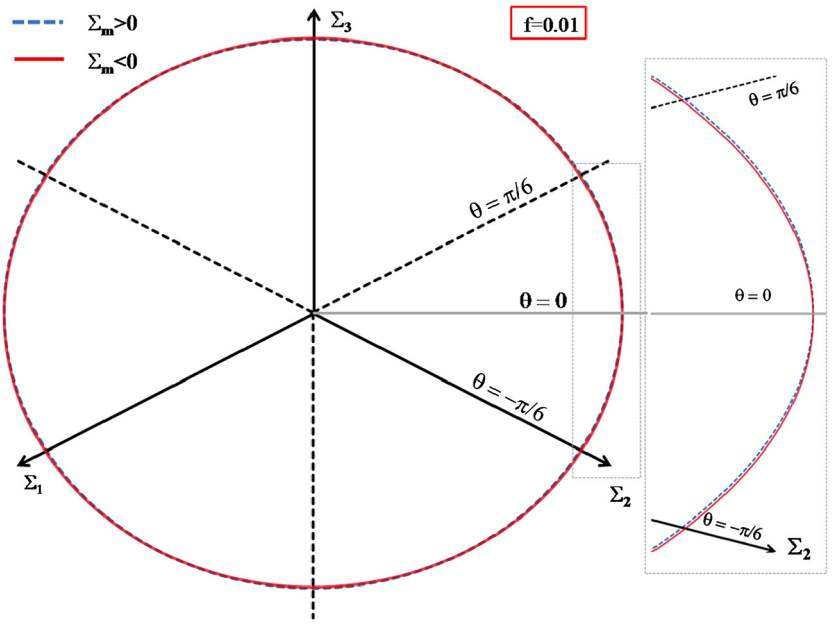

Fig. 11. (Color online.) Cross-sections of the 3-D surface for the porous von Mises material according to the new model (Eq. (29)) with the deviatoric planes $\Sigma_m/\sigma_T = +2$ (interrupted lines) and $\Sigma_m/\sigma_T = -2$ (solid lines), respectively. Note the centro-symmetry of the cross-sections due to the invariance of the plastic response to the transformation $(\Sigma_m, \boldsymbol{\Sigma}') \to (-\Sigma_m, -\boldsymbol{\Sigma}')$. Porosity: $f = 0.01$.

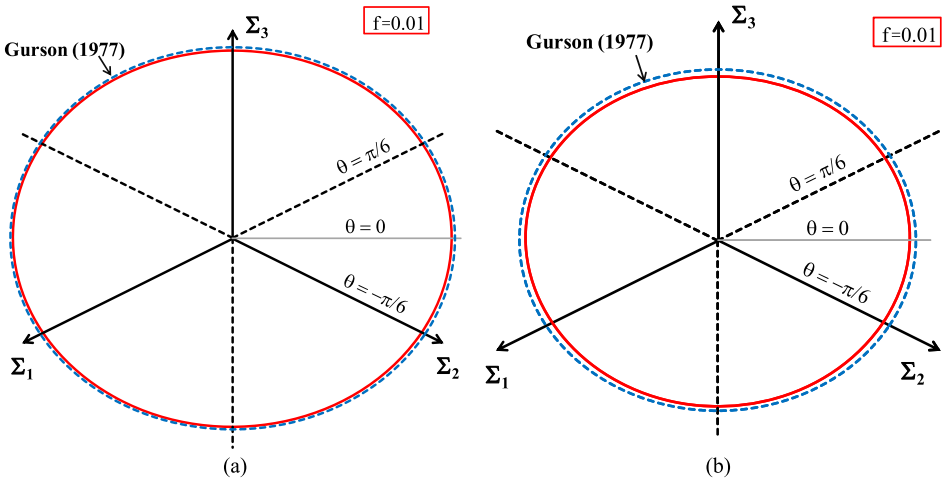

Fig. 12. (Color online.) Comparison between the cross-sections of the new 3-D yield surface (solid line; Eq. (29)) and that of Gurson's [1] yield surface (interrupted line; Eq. (1)) with several deviatoric planes: (a) $\Sigma_m/\sigma_T = 1.5$; (b) $\Sigma_m/\sigma_T = 2$. Note that Gurson's surface is external to the new surface. Initial porosity $f = 0.01$.

Although the combined effects of Σ_e and J_3^{Σ} on yielding of the porous solid are not very strong, even small differences in curvature influence the rate of void growth. Indeed, according to the criterion the direction of the normal to the yield surface depends on θ, hence the plastic flow direction and the porosity evolution are also sensitive to θ.

4. Summary and conclusions

In this paper the dilatational response of a porous material with a von Mises matrix containing randomly distributed voids was investigated using rigorous homogenization methods based on the Hill–Mandel lemma. For the first time, the analysis was conducted for general three-dimensional loadings. The strain rate based potential of the porous material was estimated. It was revealed that:

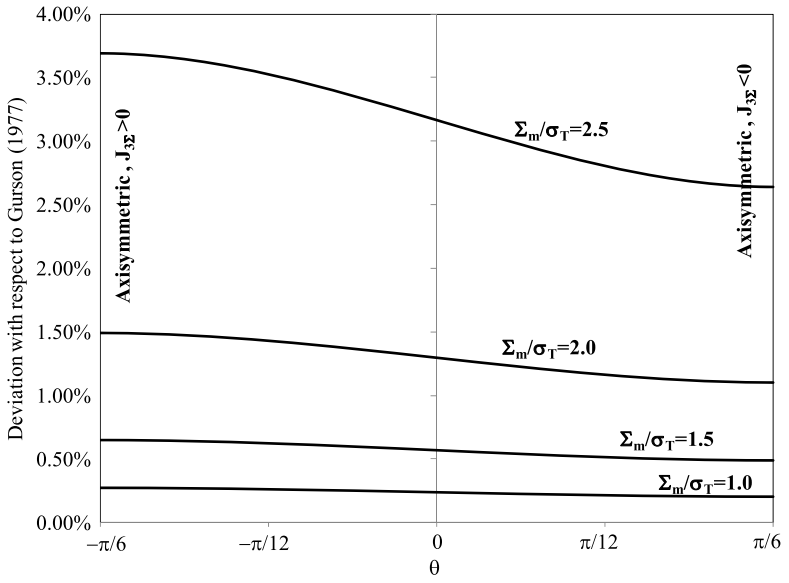

Fig. 13. Corrections brought by the new 3-D model to Gurson's [1] criterion for several levels of constant mean stress $\Sigma_m > 0$. Irrespective of the level of Σ_m, the maximum deviation is for axisymmetric states corresponding to $\theta = -\pi/6$. The highest the mean stress, the greatest is the correction to Gurson's [1] model. Porosity: $f = 0.01$.

1. the strain rate potential (SRP) of the porous Mises material should involve all three invariants of the strain rate tensor **D**;
2. the SRP is smooth, its cross-sections with the deviatoric planes have three-fold symmetry with respect to the origin, and deviate slightly from a circle;
3. the coupling between the invariants of $\mathbf{D}'$, i.e. between $R\ (=\sqrt{2J_{2D}})$ and γ (measure of $\sqrt{J_{2D}}$ and J_{3D}) is very specific:
   a. for $D_m > 0$, $R(\gamma)$ is a monotonically decreasing function of γ,
   b. for $D_m < 0$, R(γ) is a monotonically increasing function of γ;
4. the strongest effect of the third invariant is for axisymmetric states i.e. between $R(\gamma = \pi/6)$ and $R(\gamma = -\pi/6)$.

An approximate analytic strain rate potential was developed. This new potential has the following properties:

- it coincides with the exact SRP for axisymmetric states,
- since it is represented by an odd function and relies on the exact analytical values for axisymmetric states, it satisfies automatically the centro-symmetry requirement, i.e. it is invariant to the transformation $(D_m, R, \gamma) \to (-D_m, R, -\gamma)$,
- it displays three-fold symmetry with respect to the origin,
- the derivative of $R(\gamma)$ according to the new SRP with respect to γ is null for axisymmetric loadings (see Eq. (20)).

The new analytic SRP (Eq. (21)) was compared to the exact conjugate in the strain rate space of the classic Gurson [1] stress-based potential. Gurson's SRP involves only dependence of D_m and J_{2D}. Furthermore, shear and mean strain rate effects are decoupled. As a consequence, Gurson's SRP (Eq. (22)) is insensitive to the sign of the mean strain rate. Most importantly, irrespective of the level of the mean strain rate, D_m, Gurson's SRP is more dissipative than the new SRP developed in this study (Eq. (20)).

Furthermore, a new 3-D stress-based plastic potential for a porous von Mises material, that preserves all the key properties of the exact one was proposed (see Eq. (29)). The new yield criterion has the following key features:

(i) it depends on all stress invariants,
(ii) it is centro-symmetric, i.e. invariant to the transformation: $(\Sigma_m, \Sigma_e, J_3^\Sigma) \to (-\Sigma_m, \Sigma_e, -J_3^\Sigma)$,
(iii) the most influence of the third invariant of the stress deviator, J_3^Σ, on yielding occurs for axisymmetric states.

The corrections brought by this new criterion with respect to Gurson's criterion were discussed. It was shown that Gurson's [1] criterion is an upper-bound for the new criterion. Irrespective of the level of Σ_m, the most significant difference between Gurson's [1] criterion and the new criterion is for axisymmetric conditions. Furthermore, the correction brought by the new criterion to Gurson's [1] becomes more important with increasing mean stress Σ_m.

The importance of the couplings between the third invariant J_3^Σ and the second invariant Σ_e (or J_2^Σ) was also discussed. It was revealed that the influence of this coupling, or angle θ, is very small for low stress triaxialities, but there is an increasing influence of θ with increasing stress triaxiality. Irrespective of the level of the stress triaxiality T, the softest response is for axisymmetric loadings corresponding to $\theta = -\pi/6$ ($J_3^\Sigma > 0$) while the hardest response is for $\theta = \pi/6$

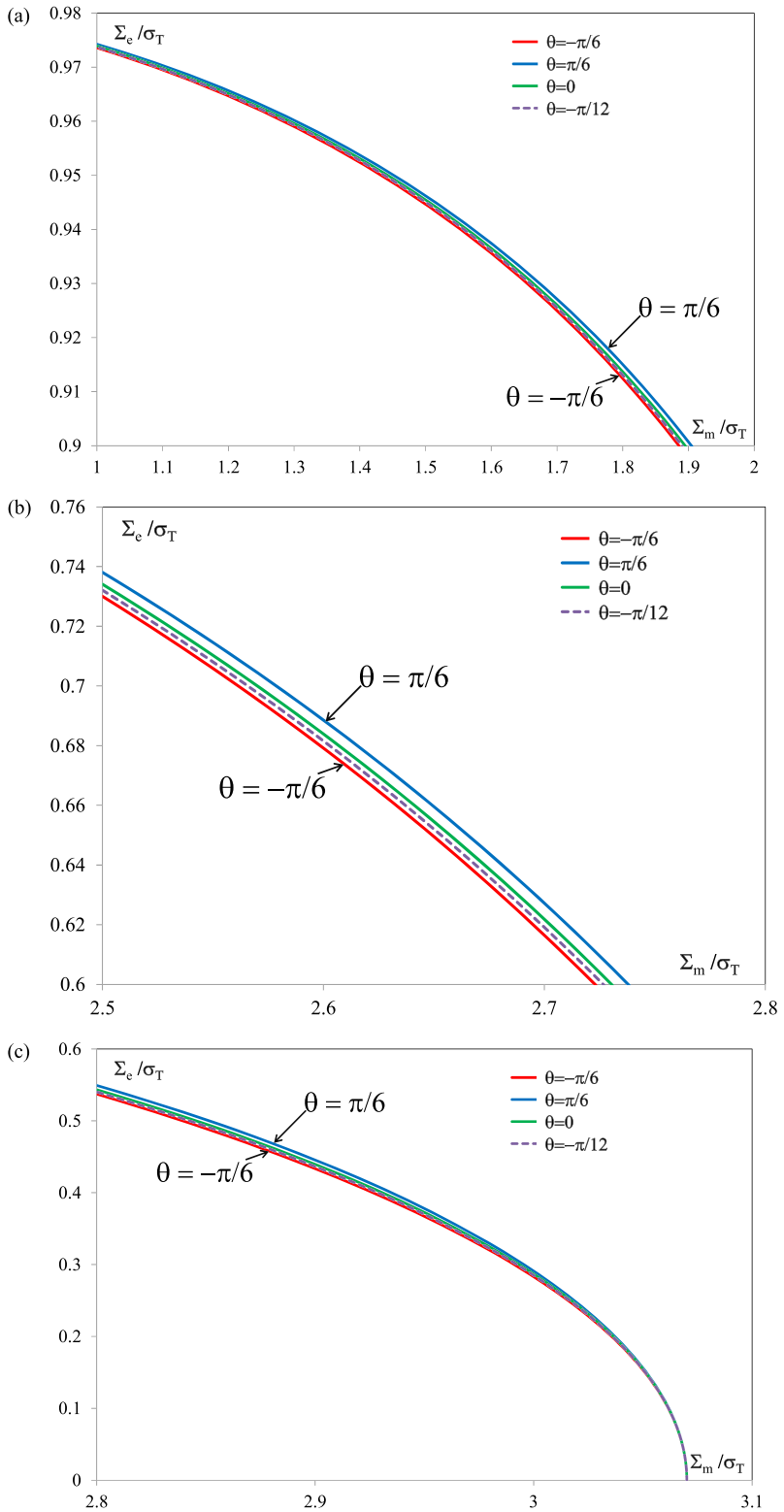

Fig. 14. (Color online.) Zoom on the tensile quadrant of the cross-sections of the 3-D surface for the porous von Mises material according to the new model (Eq. (29)) with the several planes $\theta =$ constant in the range $(-\pi/6, \pi/6)$; axisymmetric loadings correspond to $\theta = -\pi/6$ ($J_3^{\Sigma} > 0$) and $\theta = \pi/6$ ($J_3^{\Sigma} < 0$) for the following ranges: (a) low-stress triaxialities ($1 < \Sigma_m/\sigma_T, <2; 0.9 < \Sigma_e/\sigma_T < 0.98$); (b) intermediate triaxialities ($2.5 < \Sigma_m/\sigma_T < 2.8$, $0.6 < \Sigma_e/\sigma_T < 0.74$): (c) high-stress triaxialities ($2.8 < \Sigma_m/\sigma_T, <3.07; 0 < \Sigma_e/\sigma_T < 0.6$). The softest response is for axisymmetric loadings corresponding to $\theta = -\pi/6$ ($J_3^{\Sigma} > 0$), while the hardest response is for $\theta = \pi/6$ ($J_3^{\Sigma} < 0$).

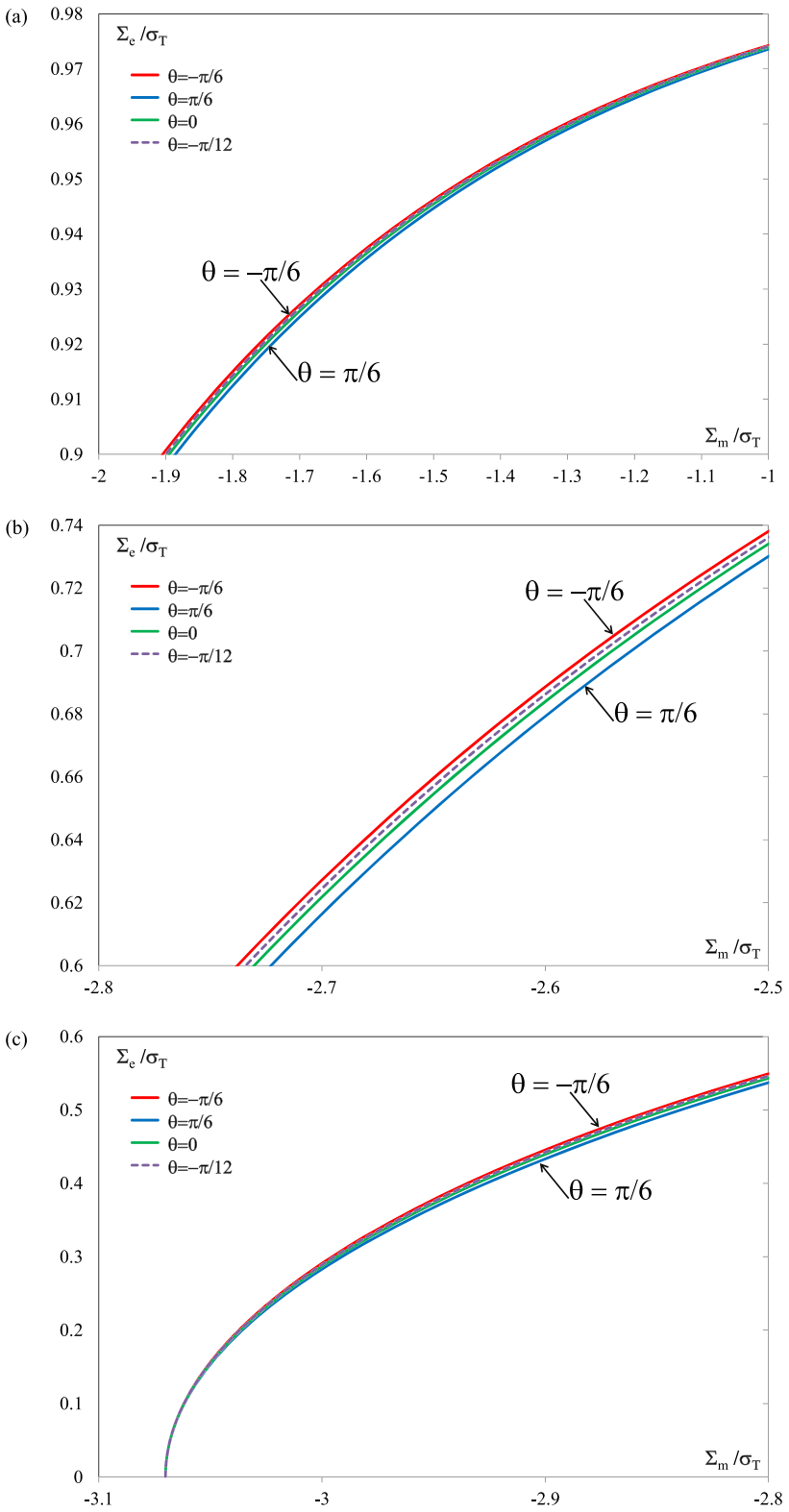

Fig. 15. (Color online.) Zoom on the compressive quadrant of the cross-sections of the 3-D surface for the porous von Mises material according to the new model (Eq. (29)) with several planes $\theta =$ constant in the range $(-\pi/6,\ \pi/6)$; axisymmetric loadings correspond to $\theta = -\pi/6$ ($J_3^{\Sigma} > 0$) and $\theta = \pi/6$ ($J_3^{\Sigma} < 0$) for the following ranges: within following ranges: (a) low-stress triaxialities ($-2 < \Sigma_m/\sigma_T < -1$; $0.9 < \Sigma_e/\sigma_T < 0.98$); (b) intermediate triaxialities ($-2.8 < \Sigma_m/\sigma_T < -2.5$, $0.6 < \Sigma_e/\sigma_T < 0.74$): (c) high-stress triaxialities ($-3.07 < \Sigma_m/\sigma_T < -2.8$; $0 < \Sigma_e/\sigma_T < 0.6$). The hardest response for axisymmetric loadings corresponds to $\theta = \pi/6$ ($J_3^{\Sigma} < 0$) while the softest response is for $\theta = \pi/6$ ($J_3^{\Sigma} > 0$).

($J_{3\Sigma} < 0$). Note that due to the centro-symmetry of the yield surface, for compressive mean stress the softest response is for axisymmetric loadings corresponding to $\theta = -\pi/6$ ($J_{3\Sigma} > 0$), while the hardest response is for $\theta = \pi/6$ ($J_3^{\Sigma} < 0$) (see Figs. 14–15).

Although the effects of the third invariant of stress on yielding seem small, its couplings with the mean stress strongly affects void evolution. It is very worth noting that the same conclusions concerning the influence of the third invariant on void evolution were drawn by Rice and Tracey [13] for the case of large triaxialities. The results presented in this paper provide fundamental understanding of the influence of all invariants on the response of isotropic porous solids. With few exceptions, the effect of the plastic anisotropy of the matrix on the dilatational response of porous solids has remained largely unexplored. In the case when the matrix is described by Hill's [16] criterion, analytic plastic potentials were deduced by Benzerga and Besson [17] for spherical void geometry; Monchiet et al. [18] for spheroidal void shape. An analytical plastic potential that accounts for the anisotropy and tension–compression asymmetry of the plastic flow of the matrix on the response of porous solids was derived by Stewart and Cazacu [19]. It is worth noting that in the derivation of the above mentioned criteria, the same restrictive hypothesis considered by Gurson (i.e. neglect the mixed terms $D_{\mathrm{m}}D'$ in the expression of the plastic dissipation) was adopted. The implications of this hypothesis on modeling anisotropic porous materials deserves further investigations.

References

[1] A.L. Gurson, Continuum theory of ductile rupture by void nucleation and growth, Part I: yield criteria and flow rules for porous ductile media, J. Eng. Mater. Tech. Trans. ASME, Series H 99 (1977) 2–15.
[2] V. Tvergaard, Influence of voids on shear band instabilities under plane strain conditions, Int. J. Fract. 17 (1981) 389–407.
[3] V. Monchiet, Contribution à la modélisation micromécanique de l'endommagement et de la fatigue des métaux ductiles, Ph.D. thesis, Université de Lille, France, 2006 (in French).
[4] A.B. Richelsen, V. Tvergaard, Dilatant plasticity or upper bound estimates for porous ductile solids, Acta Metall. Mater. 42 (1994) 2561–2577.
[5] J.L. Alves, B. Revil-Baudard, O. Cazacu, Importance of the coupling between the sign of the mean stress and the third invariant on the rate of void growth and collapse in porous solids with a von Mises matrix, Model. Simul. Mater. Sci. Eng. 22 (2) (2014) 025005.
[6] O. Cazacu, J.B. Stewart, Plastic potentials for porous aggregates with the matrix exhibiting tension–compression asymmetry, J. Mech. Phys. Solids 57 (2009) 325–341.
[7] R.A. Lebensohn, O. Cazacu, Effect of single-crystal plastic deformation mechanisms on the dilatational plastic response of porous polycrystals, Int. J. Solids Struct. 49 (2012) 3838–3852.
[8] O. Cazacu, B. Revil-Baudard, R.A. Lebensohn, M. Garajeu, On the combined effects of pressure and third invariant on yielding of porous solids with a von Mises matrix, J. Appl. Mech. 80 (6) (2013), 064501-0645015.
[9] R. Hill, The essential structure of constitutive laws for metal composites and polycrystals, J. Mech. Phys. Solids 15 (1967) 79–95.
[10] J. Mandel, Plasticite classique et viscoplasticite, Int. Centre Mech Sci., Courses and Lectures, vol. 97, Springer, Wien, New York, 1972, Udine, 1971.
[11] D.R.S. Talbot, J.R. Willis, Variational principles for inhomogeneous non-linear media, IMA J. Appl. Math. 35 (1) (1985) 39–54.
[12] A. Gurson, Plastic flow and fracture behavior of ductile materials incorporating void nucleation, growth, and interaction, PhD thesis, Brown University, Rhode Island, 1975.
[13] J.R. Rice, D.M. Tracey, On the ductile enlargement of voids in triaxial stress fields, J. Mech. Phys. Solids 17 (1969) 201–217.
[14] J. Lubliner, Plasticity Theory, Dover Publications Inc., Mineola, New York, 2008.
[15] D. Drucker, Relation of experiments to mathematical theories of plasticity, J. Appl. Mech. 16 (1949) 349–357.
[16] R. Hill, A theory of the yielding and plastic flow of anisotropic metals, Proc. R. Soc. Lond. 193 (1948) 281–297.
[17] A.A. Benzerga, J. Besson, Plastic potentials for anisotropic porous solids, Eur. J. Mech. A, Solids 20 (2001) 397–434.
[18] V. Monchiet, O. Cazacu, E. Charkaluk, D. Kondo, Macroscopic yield criteria for plastic anisotropic materials containing spheroidal voids, Int. J. Plast. 24 (2008) 1158–1189.
[19] J.-B. Stewart, O. Cazacu, Analytical yield criterion for an anisotropic material containing spherical voids and exhibiting tension–compression asymmetry, Int. J. Solids Struct. 48 (2011) 357–373.